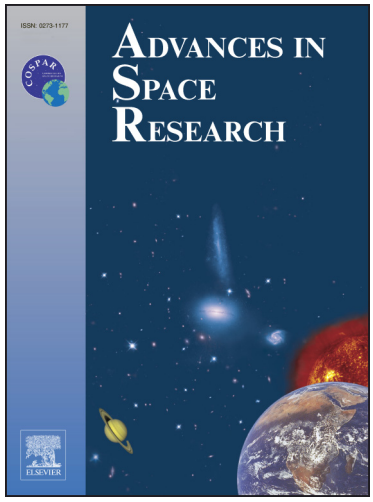

Assessment of Land Cover change and Desertification using Remote Sensing Technology in a local region of Mongolia

Munkhnasan Lamchin, Jong-Yeol Lee, Woo-Kyun Lee, Eun Jung Lee, Moonil Kim, Lim Chul-Hee, Hyun-Ah Choi, So - Ra Kim

PII: S0273-1177(15)00705-X
DOI: http://dx.doi.org/10.1016/j.asr.2015.10.006
Reference: JASR 12461

To appear in: *Advances in Space Research*

Received Date: 15 January 2015
Revised Date: 11 August 2015
Accepted Date: 6 October 2015

Please cite this article as: Lamchin, M., Lee, J-Y., Lee, W-K., Lee, E.J., Kim, M., Chul-Hee, L., Choi, H-A., Kim, S.-.R., Assessment of Land Cover change and Desertification using Remote Sensing Technology in a local region of Mongolia, *Advances in Space Research* (2015), doi: http://dx.doi.org/10.1016/j.asr.2015.10.006

Assessment of Land Cover change and Desertification using Remote Sensing Technology in a local region of Mongolia

Munkhnasan Lamchin[a], Jong-Yeol Lee[a], Woo-Kyun Lee[a]*, Eun Jung Lee[a], Moonil Kim[a], Lim Chul-Hee[a], Hyun-Ah Choi[b], So - Ra Kim[c]

[a]*Department of Environmental Science and Ecological Engineering, Korea University, Seoul, 136-713, Korea*

[b]*Hanns Seidel Foundation, Seoul Office 13 Hannamdaero 20-gil, #501 (Sooyoung Bldg., Hannam-dong), Youngsan-ku, Seoul, 140-886, Republic of Korea*

[c]*Korea Forest Research Institute, Seoul, 207 Cheongyangri-dong, Dongdaemum-gu, Seoul, 130-712, Republic of Korea*

**Author to whom correspondence should be addressed; e-mail: leewk@korea.ac.kr*

Abstract

Desertification is a serious ecological, environmental, and socio-economic threat to the world, and there is a pressing need to develop a reasonable and reproducible method to assess it at different scales. In this paper, the Hogno Khaan protected area in Mongolia was selected as the study area, and a quantitative method for assessing land cover change and desertification assessment was developed using Landsat TM/ETM+ data on a local scale. In this method, NDVI (Normalized Difference Vegetation Index), TGSI (Topsoil Grain Size Index), and land surface albedo were selected as indicators for representing land surface conditions from vegetation biomass, landscape pattern, and micrometeorology. A Decision Tree (DT) approach was used to assess the land cover change and desertification of the Hogno Khaan protected area in 1990, 2002, and 2011. Our analysis showed no correlation between NDVI and albedo or TGSI but high correlation between TGSI and albedo. Strong correlations (0.77–0.92) between TGSI and albedo were found in the non-desertification areas. The TGSI was less strongly correlated with albedo in the low and non desertification areas, at 0.70 and 0.92; respectively. The desertification of the study area is increasing each year; in the desertification map for 1990–2002, there is a decrease in areas of zero and low desertification, and an increase in areas of high and severe desertification. From 2002 to 2011, areas of non desertification increased significantly, with areas of severe desertification also exhibiting increase, while areas of medium and high desertification demonstrated little change.

Keywords: Desertification, Sand, Assessment, Correlation, Topsoil Grain Size Index

1. Introduction

Land degradation (LD) is a complex phenomenon. It reduces soil fertility (Kassas, 1999) especially in dry regions, and sometimes leads to local desertification phenomenon (Rubio and Recatala, 2006). LD causes different aspects of natural resource depletion such as degradation of soil, vegetation and water. Furthermore, LD has a negative influence on bio-physical and socio-economic processes that society has defined as important components in various spatial and temporal scales (Lal and Stewart, 1990; Puigdefabregas et al., 1998; Garcia Latorre et al., 2001).

Desertification is best to be understood as an extreme case of land degradation, which is expressed in a persistent reduction or loss of biological and economic productivity of lands (UNCCD 2010). Desertification can be also defined as "Land degradation in the arid, semiarid, and dry sub-humid areas resulting from various factors, including climatic variations and human activities" (UNCCD 1995). Globally, desertified land amounts to 3.6 × 107 km^2, which covers 24.1% of Earth's land surface and affects about one-sixth of the world's population, much of whom live in poverty (Middleton and Thomas, 1997). In recent years, the notion of desertification has been related to the loss of ecosystem services resulting from the effect of anthropogenic disturbances or climatic variations in dryland ecosystems (D'Odorico et al., 2013).

Remote sensing information with vegetation index and land surface albedo have been studied (Zeng et al., 2006; Pan and Qin, 2010). Additionally, vegetation cover is an important indicator for evaluating the extent of vegetation restoration in degraded sandy grasslands (Zhang et al., 2004). NDVI (Normalized Difference Vegetation Index) is one of the most extensively applied vegetation indices for its sensitivity to the presence, density and condition of vegetation. It is a simple numerical indicator that can be used by remote sensing measurements. NDVI provides a crude estimate of vegetation health and acts as a means of monitoring changes in vegetation over time. NDVI can be utilized as a cost effective and reliable approach for national reporting on several UNCCD core indicators. The Normalized Difference Vegetation Index (NDVI) has been most commonly used to map spatial and temporal variation in vegetation (Tucker, 1979). Thus, we have thus additionally employed NDVI as an indicator of land cover change and desertification.

The texture of topsoil is closely related to land degradation. According to Zhu et al. (1989), different extents of desertification result in different topsoil textures – the more severe the desertification, the coarser the topsoil grain composition. More recently, Fu et al. (2002) found that overgrazing can accelerate soil wind

erosion and result in topsoil coarsening. Zhao et al. (2005) showed that the sand content of a severely eroded cropland is higher than average. Coarsening of topsoil is a visible sign of land degradation, thus the grain size composition of topsoil can potentially be used as an indicator of land degradation. It is thus possible to monitor desertification by the change in Topsoil Grain Size in arid and semi-arid areas using remote sensing techniques. Topsoil Grain Size Index (TGSI) is only applicable for bare or sparsely vegetated areas. The obtained TGSI results appear to be promising for identifying and highlighting sand accumulations in the study area (Hadeel et al., 2010). The negative TGSI value indicates areas covered by vegetation, and positive TGSI represents coarse sand (Xiao et al., 2006). Given that one rainfall can significantly increase the vegetation cover, NDVI is not precise enough to indicate the actual degree of desertification. In order to develop a practical index associating the physical properties (mechanical composition) of topsoil in monitoring changes in surface soil texture using remote sensing, Xiao et al., (2006) analyzed the correlations between several of the aforementioned spectral indices and the topsoil grain size composition. The best correlation was found between TGSI and fine sand and silt-clay contents of topsoil.

Some studies showed that increasing land surface albedo implies a degradation of land quality (Riobinove et al., 1981). Clay soils can maintain high moisture content in the presence of a water supply, while sandy textured soils drain and dry out much more rapidly. Because of the differences in the resulting soil moisture content between the texture classes, there are differences in the reflectance and absorbance characteristics of the texture classes as well as the land surface albedo (Dobos, 2003). A variety of factors influence the ability of plants to reflect sunlight. At the most simplistic level, dark coloration provides the greatest absorption and hence the lowest land surface albedo. Leaf shape is quite important because leaf shapes provides reflectivity. This effect explains why conifer forests tend to have lower land surface albedo than angiosperm or broadleaf forests. Furthermore, leaf aspect is also contributory – leaves surfaces more parallel to the ground surface demonstrating higher land surface albedo (Dagmar Budikova, 2010). Land surface albedo plays a major role in the energy balance of the Earth's surface, as it defines the rate of the absorbed portion of incident solar radiation. The albedo value ranges from zero to one. A value of zero refers to a black body, a theoretical medium that absorbs 100% of incident radiation. Albedo values ranging from 0.1–0.2 indicate dark-colored, rough soil surfaces, while values around 0.4–0.5 represent smooth, light-colored soil surfaces. Albedo

varies diurnally and seasonally because of the changing angle of the sun (Dobos, 2003; Matthews, 1984; Kotoda, 1986). In general, the lower the sun's angle, the higher the albedo.

The objectives of this study are (1) to assess the land cover change and desertification process with remote sensing data (1990, 2002 to 2011) and (2) to identify a pixel-based relationship between NDVI, TGSI, and land surface albedo in the desertification grade. In this study, the study area was classified by the level of desertification, and the relationship between the desertification level and the three variables was tested; this relationship was examined by using pixel-based regression analysis.

2. Study area

The Hogno Khaan nature reserve is located between the 47°23′ and 47°38′N latitudes and the 103°30′ and 103°50′E longitudes. It is the region of Khangai-Khentii ranges, and this reserve shares the boundaries of three different geographic regions in Mongolia. The nature reserve covers 835.45 km^2 of land, and is situated in the area of Gurvanbulag and Rashaant sums of Bulgan Province, and Burd sum of Uvurkhangai Province. The Elsen Tasarkhai sand dune, located in this area, comprises the Mongol Els in the south and the Hogno Tarnyn Els in the north. Elsen Tasarkhai sand is sodden under its surface, therefore, *shrubberies* such as *Ulmus pumila*, *Salix ledebouriana* grow in the area. The Elsen Tasarkhai sand is surrounded by mountains Hogno Khaan to the north and mountains Ikh Mongol to the south (Figure 1). This area contains various geomorphic and topographic features including high mountains, steppes, sand dunes and a river under a continental climate. Geologically, high mountain are composed of Jurassic granites and the topography is characterized by rocky outcrops and flat or rounded slopes with the highest peak of 1967 m above sea level and Tarna river basin and depressions at 1165.

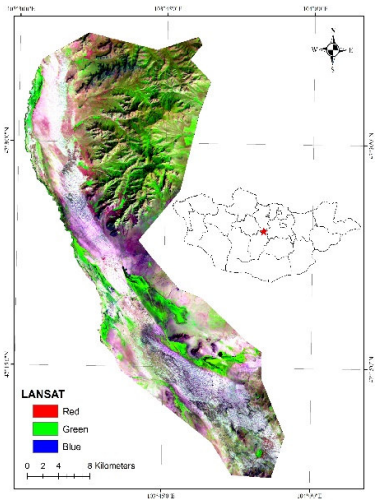

Figure 1. Geographic location of the study area and Landsat TM image of RGB band composition taken on August 17, 2011

This area was taken under state protection in 1997 by Parliament Resolution No.47. The Hogno Khaan area is characterized by an extreme continental climate, dry and cool.

The temperature varies from -20°C ~ -25°C in the winter, to 20°C ~ 27°C in the summer. The coldest month is January, with the lowest recorded temperature of about -44°C, while the warmest is July, with a recorded high of 30°C. Mean annual precipitation in the area is 250 to 300 mm, 80 ~ 90% of which is recorded in the warm season.

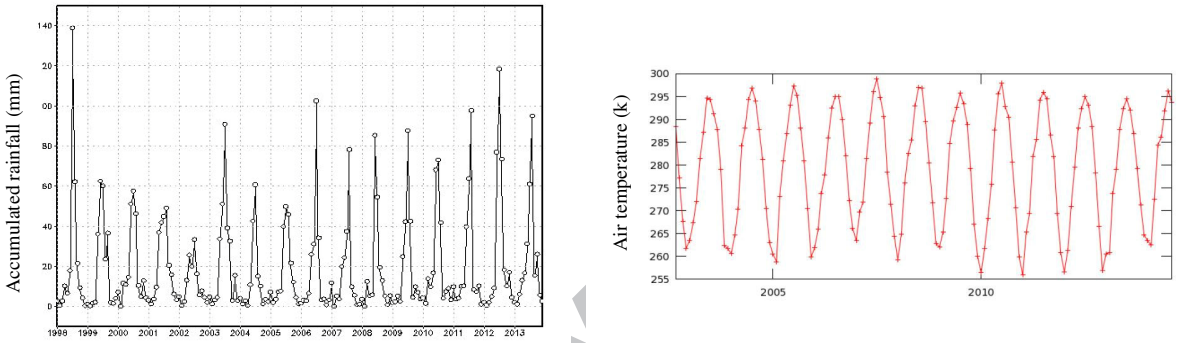

Figure 2. Graph of yearly rainfall (1990-2014) and air temperature (2003-2014) of study area generated by NASA's Giovanni.

The wind velocity ranges from 0.5 to 2.3 m/s, with the maximum occurring in May at about 4.0 m/s. Lens of permafrost, as well as seasonal frosts, occur in the intermountain valley bottoms and on the north-facing slopes for 5–5.5 months, and their depth ranges between 3.2 and 4.5 m. A vast sand dune is distributed on the western margin and southwestern corner of the protected area. This is an Aeolian dune, extending south and north along the valley due to the deflation of dune crests in the Tarna-Tuul region. Different types of vegetation occur, according to the stability of the sand dune: (1) *Polygonum-Oxytropis* herb communities in the beginning stage of dune formation, (2) *Salix* shrub communities in the early pioneer stage, and (3) *Betula* shrub communities in the later pioneer stage. Among these, the *Betula* shrub community dominates the most stabilized sand dunes. Two shrub communities of *Salix sp.* and *Betula sp.* show a bushy and mono-dominated physiognomy. Cutting for firewood is the main disturbance factor for the shrubs. A wide terrace carved by channel incisions is found in the Schiluust streamlet of the Tarna River. The floodplain of the stream channel at base flow is about 15 m wide, the bankfull channel (thalweg) is 1 m wide and 0.2 m deep, and the scarp slope is

very sharp. *Iris bungei* communities are typical on the sandy soil of the wide terrace, and show the effects of overgrazing in dry grasslands in the semi-desert zone.

3. Materials and methods

3.1. Materials and preprocessing

In this research, the progress of desertification in the Hogno Khaan protected area was evaluated using seven periods of satellite remote sensing images between 1990 and 2011. Landsat ETM+ (Enhanced Thematic Mapper Plus – Landsat 7) image recorded on August 16, 2002, August 21, 1995, July 23, 1999 (path/row 133/027), and Landsat TM (Thematic Mapper – Landsat 4–5) images recorded on September 8, 1990, September 4, 2006, August 20, 2010 and August 17, 2011 (path/row 133/027). These images, provided by the website http://landsat.usgs.gov, are cloud free. This research used seven years satellite data in multi temporal changes of three variables and classified desertification map using three years data. The 6S method of atmosphere correction was used, which predicts the reflectance (P_p) of objects at the top of atmosphere (TOA) using information about the surface reflectance and atmospheric conditions (Vermote *et al*., 1997). This information is provided through a minimum of input data to the model and incorporated features. The TOA reflectance can be estimated using the following formula:

$$P_p = \frac{\pi L_\lambda d^2}{(ESUN)_\lambda \cos\theta_S}$$

where P_p is the planetary reflectance, π is 3.14159, L_λ is the spectral radiance at the sensor's aperture, d is the Earth–sun distance in astronomical units, $(ESUN)_\lambda$ is the mean solar exoatmospheric irradiance, and θ_s is the solar zenith angle in degrees.

3.2. Processing of images

Changes of the land surface conditions are closely related to desertification. Main characteristics of the desertification are soil degradation, micrometeorological alteration, declining of land cover and vegetation

biomass. The three indicators, NDVI, TGSI and land surface albedo are assessing components of desertification in this study.

The software packages used for this study were ENVI for image processing, Arc/info was used for analyzing and presenting the results, and statistical and graphical SPSS was used for statistical analysis.

1. ***Normalized Difference Vegetation Index (NDVI):*** The most common form of vegetation index is the Normalized Difference Vegetation Index (NDVI). The NDVI is the difference between the red and near-infrared band combination divided by the sum of the red and near-infrared band combination:

$$NDVI = \left(NIR_{b4} - R_{b3}\right) / \left(NIR_{b4} + R_{b3}\right) \quad (2)$$

where R and NIR are the red and near-infrared bands.

2. ***Topsoil Grain Size Index (TGSI):*** Topsoil Grain Size Index (TGSI) was developed based on the field survey of soil surface spectral reflectance and laboratory analyses of soil grain composition (Xiao et al., 2006). Even one rainfall can significantly increase the vegetation cover. Thus, NDVI is misinterpret the actual degree of desertification (Xiao et al, 2006). To overcome this problem, Xiao et al. (2006) proposed a new index, topsoil grain size index (TGSI), which is associated with the mechanical composition of topsoil. It indicates the coarsening of topsoil grain size which has a positive correlation with fine sand content (this class of sand is dominated by the finer sizes of sand particle, and somewhat less coarse than either sand or coarse sand) of surface soil texture, as a manifestation of undergoing desertification. The more severe the desertification, the coarser the topsoil grain size composition (grain size refers to the mean or effective diameter of individual mineral grains or particles. A high TGSI value corresponds to an area with high content of fine sand in the topsoil or low content of clay-silt grains. The TGSI can be calculated as

$$TGSI = \left(R_{b3} - B_{b1}\right) / \left(R_{b3} + B_{b1} + G_{b2}\right) \quad (3)$$

where *R*, *B*, and *G* are the red, blue, and green bands of the remote sensing data, respectively. TGSI is an index used to detect the texture of the topsoil layer, or grain size. Negative values or those near 0 represent zones with vegetation or water bodies and values near 0.20 indicate high contents of fine sand (Xiao et al., 2006).

3. ***Albedo:*** Land surface albedo is an important indicator that determines the energy budget and change in micrometeorological conditions such as the temperature and aridity/humidity of the land affected by

desertification (Li et al., 2000; Jackson et al., 1975). Some studies have shown that increasing land surface albedo implies a degradation of land quality (Riobinove et al., 1981). In this study, we used the broad-band albedo, which is determined by the combination of narrow-band albedo, to assess the micrometeorological conditions on the land surface. The narrow-band albedo for each band (except band six for Landsat TM/ETM+) of Landsat images was determined using the dark object subtraction method (Chavez et al., 1988; Chavez et al., 1996). The broad-band albedo was then calculated according to its relationship with each narrow-band (Musick, 1986; Liang, 2001; Smith, 2010). The broad-band albedo calculation for Landsat TM/ETM+ is expressed by:

$$Albedo = 0.356 B_{b1} + 0.130 R_{b3} + 0.373 NIR_{b4} + 0.085 SWIR_{b5} + 0.072 SWIR2_{b7} - 0.0018 \quad (4)$$

where *Albedo* represents the broad-band albedo of Landsat TM/ETM+, and $b1–7$ are the narrow-band albedo for each band of Landsat TM/ETM+.

We computed Albedo by transforming digital numbers (DN) of Landsat ETM+ and Landsat TM images into values to Top of Atmosphere (TOA) reflectance images. It is possible to convert these DN to TOA Reflectance using two steps process. The first step is to convert the DN to radiance values. The second step converts the radiance data to TOA reflectance.

3.3. Assessment Method

In this study, the land desertification of Hogno Khaan was classified into five grades: zero desertification, low desertification, medium desertification, high desertification, and severe desertification according to a frequently used grading system in Mongolia. Our goal was to separate each desertification grade using the differences among the indicators and the combinations of land desertification. The Decision Tree (DT) is a suitable approach for classification. It can employ tree-structured rules recursively to partition the data set feature spaces into increasingly homogenous classes based on a splitting criterion (Duanyang et al., 2009). DT classification has been used for vegetation mapping and soil mapping in remote sensing studies (Friedl and Brodly, 1997; Rogan et al., 2002). According to the frequency distribution of the five desertification grades for each vegetation sub-region in a certain period, the rules for each indicator can be established, and a DT can be constructed (Xu et al., 2009). In their study, they used DT classification to assess the status of desertification of

Ordos. They used the following three indicators: NDVI, MSDI (Standard Deviation Index), and land surface albedo.

The information of ancillary data sources are help to improve assessment of desertification, especially in large area land-cover mappings that involve cover types characterized by high levels of within-class variability (Mclver and Friedl, 2002). We used vegetation type, soil map and land cover ancillary information for assessing land cover change and desertification at local scale. In addition, the date of image be served as ancillary data due to variations of indicators for a desertification grade at different times in a year.

Bayasgalan (2005) studied vegetation trends in Mongolia for using long-term remotely sensed NDVI (1982-2003). She calculated NDVI criteria for main 6 natural zones of Mongolia and used natural zones map (Dash and Dorjgotov, 2002). We classified NDVI by this criteria as table.

Table 1. NDVI criteria of Mongolia (Bayasgalan, 2005).

NDVI values	Natural zones
0.01 – 0.15	Desert
0.15 – 0.30	Desert steppe
0.30 – 0.45	Steppe
0.45 – 0.60	Forest steppe
0.60 – 0.75	High mountains
0.75 – 1.00	Tundra

In this study, we used DT classification for assessing and land cover change and desertification usingvariables NDVI, TGSI, and land surface albedo (Figure 3).

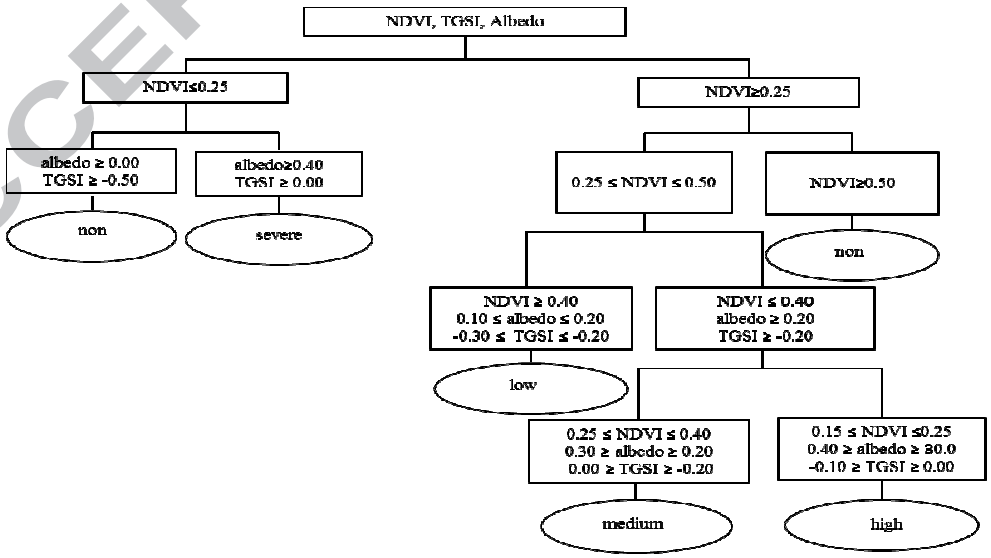

Figure 3. The Decision tree diagram for assessing and classifying desertification grade using NDVI, TGSI, and albedo.

According to frequencies distribution of the five desertification grade for each vegetation and land cover in a certain period, the rules can be established in the way of DT.

3.4 Linear correlation and regression analysis

Pearson's correlation coefficients were used for an correlation between NDVI, TGSI, and land surface albedo. The regression equations established a causal correlation between dependent (NDVI) and independent (TGSI and albedo) variables, and allowed the calculation of predicted values for 5 × 5 pixels. The analysis can be performed by the linear regression method using one variable, $y = a + bx$. Here, x is independent (TGSI and land surface albedo), and y is a dependent variable (NDVI). We calculate the slope of the correlation using a program written in FORTRAN.

Regression Equation(y) = a + bx, NDVI=a+b(TGSI*Albedo)

a = The intercept point of the regression line and the y axis.

b = The slope of the regression line

x and y are the variables.

4. Results and discussion

4.1. NDVI, Topsoil Grain Size Index and Albedo

In Table 2, NDVI, TGSI and Albedo images were compared in terms of minimum, maximum, mean, and standard deviation of time series images during the last 20 years. The change in intensity of NDVI fluctuated during the following periods: 1990 (max was 0.65, min was -0.04), 2002 (max. = 0.51, min. = -0.13), and 2011 (max. = 0.73, min. = -0.34). The minimum values in NDVI increased between -0.04 and -0.34, and TGSI decreased between -0.67 and -0.42 during these years. Furthermore, the TGSI images showed a decreasing tendency in the maximum values.

TGSI value fluctuated during the following periods: 1990 (max. = 0.36, min. = -0.67), 2002 (max. = 0.16, min. = -0.17), and 2011 (max. = 0.02, min. = -0.42). This indicated that the dominant soil particle size changed. The dominant soil particle class changed from clay silt to a combination of very fine sand in the hills area, and from very fine sand to fine sand in the low elevation area.

Table 2. Changed for distributions of NDVI, TGSI and Albedo changes

Variable	Year	Min	Max	Mean	St. Dev
NDVI	1990	-0.04	0.65	0.12	0.16
	1995	-0.05	0.73	0.10	0.15
	1999	-0.13	0.67	0.05	0.10
	2002	-0.13	0.51	-0.003	0.04
	2006	-0.16	0.63	0.08	0.11
	2010	-0.29	0.71	0.09	0.13
	2011	-0.34	0.73	0.11	0.15
TGSI	1990	-0.67	0.36	-0.10	0.12
	1995	-0.50	0.02	-0.09	0.11
	1999	-0.21	0.17	0.01	0.04
	2002	-0.17	0.16	0.02	0.04
	2006	-0.45	0.01	-0.06	0.08
	2010	-0.45	0.02	-0.06	0.08
	2011	-0.42	0.02	-0.07	0.09
Albedo	1990	0.00	0.59	0.14	0.15
	1995	0.00	0.61	0.15	0.16
	1999	0.00	0.65	0.16	0.19
	2002	0.00	0.67	0.17	0.20
	2006	0.00	0.64	0.16	0.18
	2010	0.00	0.64	0.16	0.18
	2011	0.00	0.62	0.15	0.17

The maximum value in the NDVI, TGSI, and albedo values was observed in 2002, whereas the minimum was observed in 1990 (Figure 4). It should be noted that a severe drought occurred in 2002, and the three indices were reduced in the mountainous areas. NDVI values were between 0.60 and 0.75, TGSI values were between -0.5 and 0.4, and the albedo values were between 0.0 and 0.1.

In areas where the degree of desertification was low, the NDVI values were high, whereas the TGSI and albedo values were low. However, in areas of high desertification, NDVI values were low, and the TGSI and albedo values were high. In the past 20 years, NDVI has decreased in the southern part, where TGSI and albedo has increased. Figure 4 shows a high TGSI value area concentrated on the northwest and southern region in 2002 and 2011, where the TGSI value decreased during the later years – this indicates that the fine sand content of the topsoil was decreasing. In contrast, clay and silt were found to be increasing in this direction. In the higher, northeast hill area, there are fewer fine grains (clay and silt) in the surface soil, and the TGSI values appeared low. Correlation analysis indicated significant positive correlation between TGSI and land surface albedo at all levels of desertification (Table 3). The coarse sand, fine sand, and silt–clay contents distribution is one of the most important factors in desertification reversal. Xiaohong Chen et al. 2009 conducted correlation analysis which indicated a significant negative correlation between the coarse-fine sand content and soil nutrient

content in contrast with significant positive correlations for very fine sand content and silt clay content. This can imply that changes in soil nutrients and their availability were controlled by the soil texture; also, that the particle size distribution was one of the most important factors in desertification reversal. Calculated values of the three variables vary by grade of desertification. Specifically, in areas of zero desertification, NDVI was characterized by values of 0.45–0.75, TGSI by values of -0.50–0.30, and albedo by values of 0.00–0.10. In areas of low desertification, NDVI values were 0.30–0.45, TGSI values were -0.30–0.20, and albedo values were 0.10–0.20. In contrast, areas of medium desertification were characterized by NDVI values of 0.15–0.30, TGSI values of -0.20–0.10, and albedo values of 0.20–0.30. The results showed that in 1995 areas of high NDVI values demonstrated high humidity, whereas in 2002 the low value areas exhibited drought; these findings are important given that change in vegetation cover is quite sensitive to rainfall.

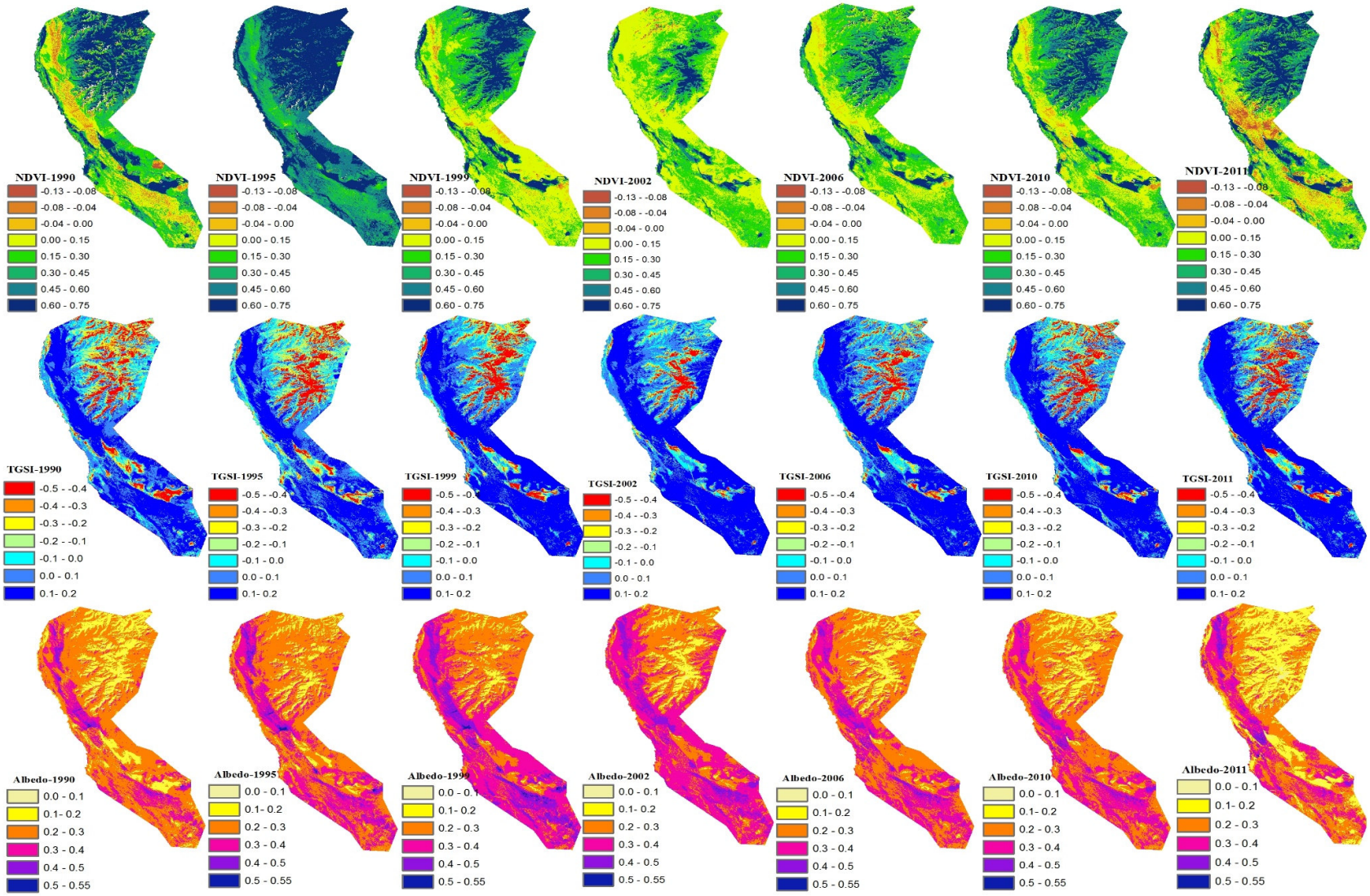

Figure 4. a) NDVI, b) TGSI, and c) Albedo of map by each year

4.2. Linear correlation and regression analysis

Linear correlations between NDVI, TGSI and land surface albedo were calculated for each desertification grade. Our analysis showed no correlation between NDVI and albedo or TGSI, but the highest correlation between TGSI and albedo. Strong correlations (0.77–0.92) between TGSI and albedo were found in the zero desertification areas. The TGSI was less strongly correlated with albedo, and were 0.70 and 0.92 in the low and zero desertification areas; respectively. The coefficient ranges represented the following correlations between TGSI and albedo: 0.39–0.48 in medium desertification areas, 0.38–0.69 in high desertification areas, and 0.33 in severe desertification areas (Table 3).

According to the rule sets, the changes in NDVI and albedo had a linear correlation with the change in desertification grade, showing the reversal of desertification characterized by increasing NDVI or decreasing albedo and TGSI. The rule sets for different desertification grades varied greatly by correlation, especially between NDVI and albedo; and NDVI and TGSI – these correlations demonstrated higher NDVI values and lower albedo and TGSI values for each year (Table 3).

Table 3. Linear correlations of three factors by desertification grade for each year

1990	Correlation	Non grade	Low grade	Medium grade	High grade	Severe grade
	NDVI and TGSI	-0.20	-0.38	-0.38	-0.57	-0.28
	NDVI and albedo	-0.06	-0.21	-0.34	-0.58	-0.34
	Albedo and TGSI	0.77	0.72	0.45	0.69	0.33
2002	NDVI and TGSI	-0.53	-0.30	-0.25	-0.17	-1.00
	NDVI and albedo	-0.39	-0.57	-0.30	-0.46	-0.46
	Albedo and TGSI	0.92	0.73	0.48	0.57	0.07
2011	NDVI and TGSI	-0.34	-0.51	-0.37	-0.41	-0.36
	NDVI and albedo	-0.12	-0.20	-0.25	-0.30	-0.31
	Albedo and TGSI	0.80	0.70	0.39	0.38	0.33

Figure 5 illustrates that the correlation analysis indicates a significant, mostly negative correlation between NDVI and albedo versus significantly lower, positive (0.00–0.10) correlations for 2002 over a small area. This indicates decreased NDVI values and even lower decreasing albedo values, which in turn indicates dark-colored soil surfaces in this area.

Comparable results, with higher negative correlation between NDVI and albedo, were found for 2011 compared to 1990. The albedo indicated grasslands and clayey silt, soil in this region in 1990, but in 2011 this region was covered by dark-colored soil surfaces, in which the albedo values were low (0.1–0.2); the grasslands had slightly higher albedo values (0.1–0.25).

In general, the degree of negative correlation between NDVI and albedo, and the correlation between NDVI and TGSI, increased from the areas of severe desertification to areas of non-desertification. When comparing areas with correlation coefficient values of 0.00–0.10 and 0.10–0.20, significant correlations between TGSI and albedo were identified in areas of severe, high, and medium desertification. An overwhelming proportion of the study area had coefficient values in the range of 0.00–0.10 and 0.10–0.20 (Figure 5).

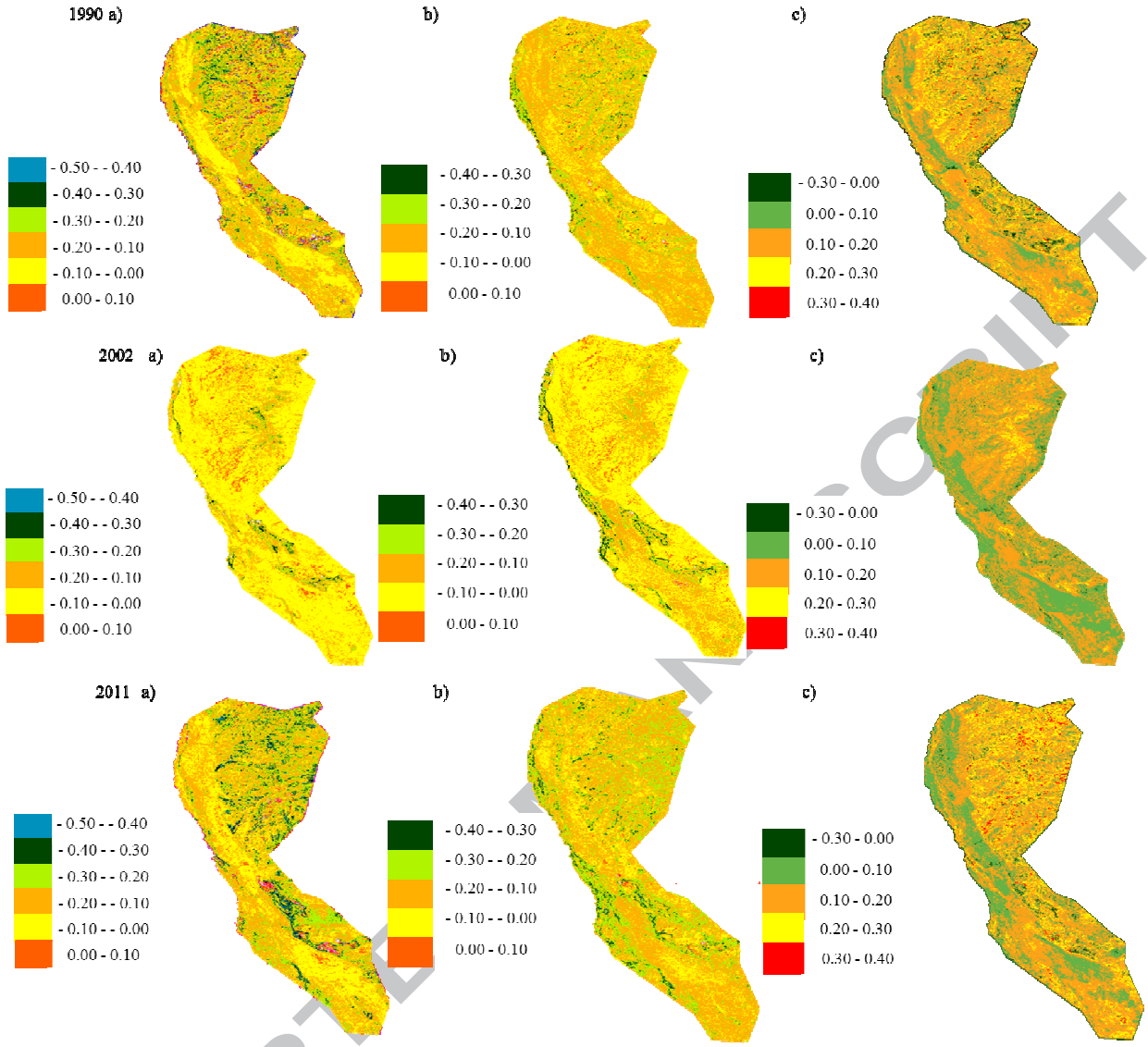

Figure 5. Slope of correlation between NDVI, TGSI, and albedo. a) Slope of correlation between NDVI and albedo. b) Slope of correlation between NDVI and TGSI. c) Slope of correlation between TGSI and albedo.

4.3. Assessment of desertification

The rule sets of indicators for each grade of desertification in the study area are listed in Table 4. For each of the five grades of desertification of the study area the following values were found for the three variables. Great differences exist for defining a desertification grade from the three indicators on a local scale. The three previous indices were used together to assess the desertification on the basis of the calculated desertification grade.

Table 4. Rule sets for desertification assessment using Landsat TM/ETM+ images

Desertification grade	NDVI	TGSI	Albedo
non	0.75 – 0.50	-0.50 - - 0.30	0.00 – 0.10
low	0.50 – 0.40	-0.30 - - 0.20	0.10 – 0.20
medium	0.40 – 0.25	-0.20 - - 0.10	0.20 – 0.30
high	0.25 – 0.15	-0.10 - - 0.00	0.30 – 0.40
severe	0.15 – 0.00	0.00 - 0.20	0.40 – 0.55

"non", "low", "medium", "high" and "severe" are used to represent desertification grades

Table 5 shows the distribution of desertification grades in the study area. It is clear that most of the study area showed high desertification; these classes occupied 298.58 km^2 (35.7%) of the total area in 2011. Desertification maps were generated for three years (Figure 6), and the individual class area and change statistics for the three years are summarized in Table 5. From 1990 to 2002, the high desertification area increased by approximately 48.99 km^2 (5.9%), while the non desertification area decreased by 12.65 km^2 (0.7%), the low desertification area decreased by 41.5 km^2 (5.4%), and medium desertification area decreased by 2.71 km^2 (0.3%). The high and severe desertification areas increased by 1.3% from 1990 to 2002, with the greatest increase occurring from 2002 to 2011, while the areas of non and low desertification decreased by 2.1% and 6.8%, respectively.

The desertification of the study area is increasing each year. In the desertification map for 1990–2002, there is a decrease in areas of non and low desertification, and an increase in areas of high and severe desertification. From 2002 to 2011, the areas of non desertification increased significantly, areas of severe desertification also increased, while areas of medium and high desertification saw little change.

Table 5. Summary of desertification for 1990, 2002, and 2011

Desertification	1990				2011		Percent change,	Square of change
grade	Area (km^2)	%	Area (km^2)	%	Area (km^2)	%	1990–2011 (%)	1990–2011 (km^2)
Non	107.25	12	94.60	11.3	88.54	10.5	-2.2	-18.7
Low	216.45	25.9	171.97	20.5	149.78	17.9	-7.9	-66.6
Medium	219.31	26.2	216.60	25.9	170.38	20.3	-5.8	-48.9
High	231.98	27.7	280.97	33.6	298.58	35.7	7.9	66.6
Severe	60.46	7.2	71.31	8.5	128.17	15.3	8.1	67.7

The dominant land cover types in this region are sand dunes and grasslands. Since the 1990s, there have been desolate croplands, however neglect cropland areas have increased since 2000. During the last ten years, degraded areas have increased dramatically. In the south and northwest part of Hogno Khaan have seen an expansion of desertification, the trend of desertification in these areas during the last twenty has gradually increased in different grades of desertification. Cultivation of planted crops in some agricultural zones in 1980–1990 resulted in degraded soil and abandonment of the fields in 1990–2000. As a result, *Chenopodium album L, Caragana microphylla, Urtica cannabina L*, *Artemisia Adamsii, Artemisia frigida, Potentilla bifurca, Potentilla anserina., Carex duriuscula, Agropyron cristatum* started to grow in these areas, which indicated the ongoing process of the desertification. However, these regions show a medium NDVI value because those plants reflect green color – this demonstrates that NDVI value can be used to indicate change in 'greenness'.

As indicated in Table 5, non, low, and medium desertification level was decreased; high and severe desertification increased by about 8% during the last 20 year. This region is a protected area that is covered by natural sand dunes and experiences increased sand movement. Also, this region has shown areas of non desertification converting into areas of low desertification and areas of medium and high desertification becoming areas of severe desertification.

Figure 6. Desertification maps of Hogno Khaan protected area in 1990, 2002, and 2011.

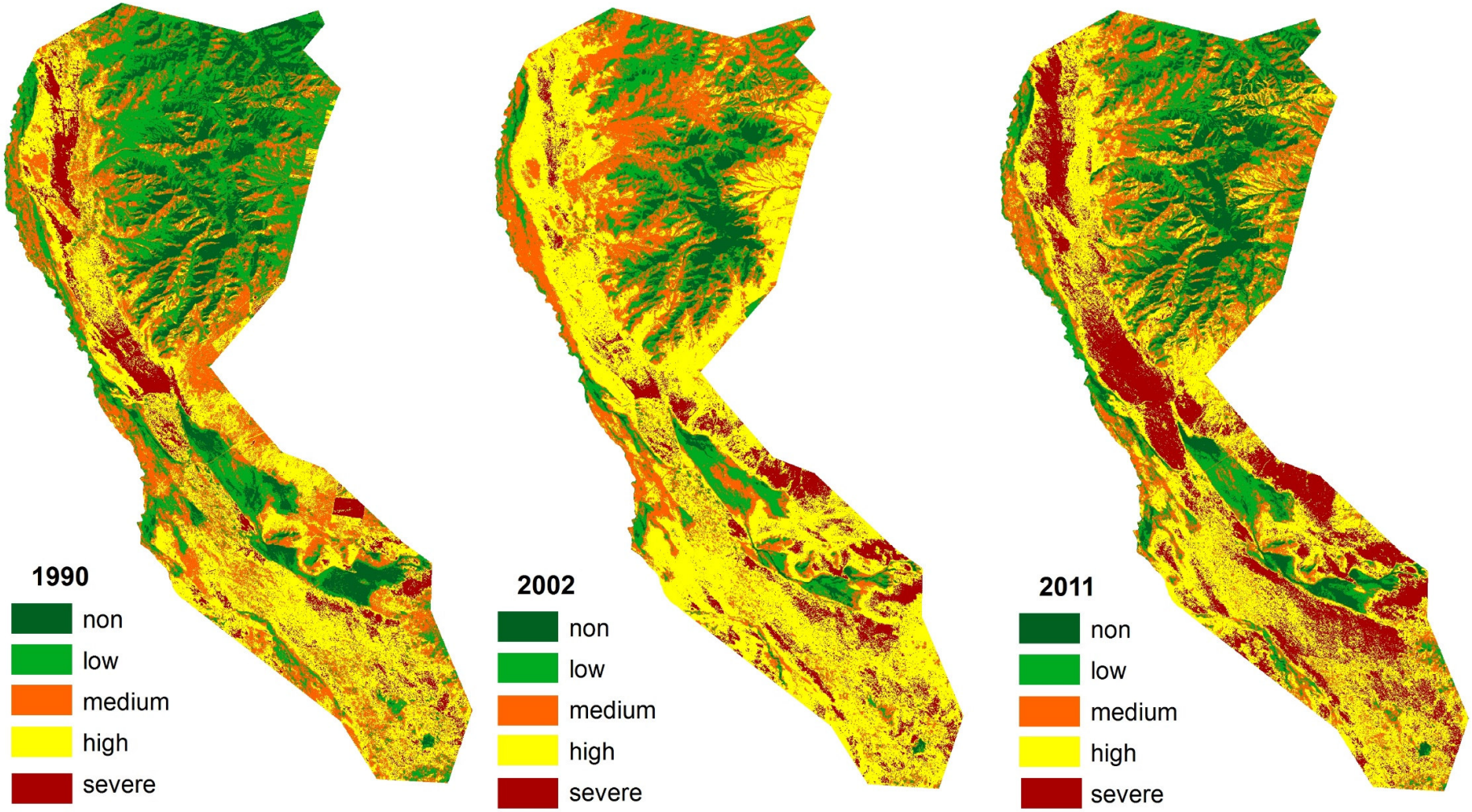

To further evaluate the results of desertification conversions, matrices of desertification changes from 1990 to 2011 were created (Table 6). In table 6, unchanged pixels are located along the major diagonal of the matrix. The period between 1990 and 2011 witnessed a conversion of more than 36.28 km^2 of zero desertification area into low desertification area, 79.8 km^2 of low desertification area into medium desertification area, and 108.95 km^2 into high desertification area. Conversion values are sorted by area and listed in descending order.

These results indicate that increases in high desertification areas mainly came from conversion of low desertification areas to medium desertification during the ten-year period, 1990–2011. Furthermore, 92.58 km^2 of high desertification area was converted to severe desertification area between 1999 and 2011, while at the same time, 15.31 km^2 area of medium desertification was converted to severe desertification.

Table 6. Matrices of desertification and changes from 1990 to 2011 (area in km^2)

1990	2011					
	Non	Low	Medium	High	Severe	Total
Non	68.12	36.28	2.17	0.60	0.08	107.26
Low	19.56	98.30	79.08	18.84	0.67	216.45
Medium	0.78	14.3	79.96	108.95	15.31	219.32
High	0.07	0.79	8.49	130.05	92.58	231.98
Severe	0.01	0.09	0.68	10.15	49.53	60.46
Total	88.54	149.78	170.38	268.59	158.17	835.45

Although similar statistics could be generated for the change statistics, they would shed little light on the question of where desertification changes are occurring. However, by constructing a change detection map (Figure 7), the advantage of satellite remote sensing in spatial disaggregation, allows the change statistics to be fully appreciated. Figure 7 shows a map of the desertification change and the conversion type (decrease, increase, or no change). Conversions involving these three classes also represent the most significant changes. A surplus of high and severe desertification and the loss of non, low, and medium levels of desertification are the most important conversions in this area.

The most significant factors affecting land surface albedo are the type and condition of vegetation covering the soil surface, soil moisture content, organic matter content, particle size, iron-oxides, mineral composition, soluble salts, and parent material (Duanyang et al., 2009). The land surface albedo for grassland and cropland ranges between 0.1 and 0.25 (Jones, 1992; Jensen et al., 1992; Oke, 1978; Van Wijk, 1963). The higher the soil moisture content shows darker the color, and the lower the albedo.

In this area, desertification related with slope and elevation. Furthermore, there are many herders moving to and around rivers and wells on lowlands. Higher slope areas facilitate higher run-off allowing less residence time for rainwater, whereas in gentle slope areas the surface run-off is slow, allowing more time for rainwater to percolate and hence undergo comparatively more infiltration. The eastern part comprises rolling hills with slopes exceeding 8% and can reach as high as 40%. The south part of the study area was characterized by undulating plains with slopes ranging from low.

From ancient times to the present day, pastoral livestock production has been one of the main agricultural activities in the study area. In the Hogno Khaan, where more than 60% of its territory is occupied by pastureland and about 20% by sand, the main land use is nomadic livestock breeding and grazing. The first and most sensitive parameter to respond to that stress is the pasture natural vegetation, which is an important resource in this historic nomadic pastureland; the second parameter is climate activity. In other words, the sand dune area was expanding according to wind speed in the spring season.

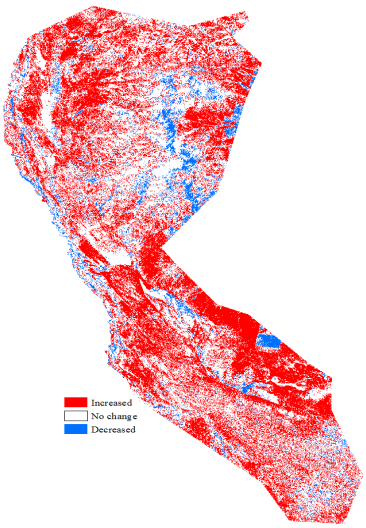

Figure 7. Desertification change map between 1990 and 2011

During the last 20 years, the data shows that the area of high value of TGSI had increased, and the areas with low TGSI had decreased. The albedo value has been increasing year by year (Figure 4). We hypothesize that the dominant soil particle class changed from clay silt to a combination of very fine sand in the hills area, but turned into very fine sand to fine sand in the topsoil of low elevation areas. Given that the smaller particles are highly vulnerable to wind erosion, this change reflects the intensity of wind erosion, increasing the

volume of shifting sands. The results from change detection indicate the reduction of desertification level of the study area (Figure 7).

In contrast, from 2002 to 2011, the areas with medium and high desertification decreased, but the areas with high and severe desertification expanded (Figure 7). Sand dunes are included at level of severe desertification according to the results. We hypothesize that the expansion of high and severe desertification areas reflects sand movement. Desertification usually experiences the following three stages: (1) conversion from fixed sand dunes to semi-fixed sand dunes due to removal of vegetation, (2) conversion from semi-fixed dunes to semi-moving dunes, and (3) conversion from semi-moving dunes to moving sand dunes. Desertification and frequent sand storms in the spring strongly affect the growth of grassland vegetation and crops, and usually lead to large losses in yield as a result of wind erosion and sand dune movement (Liu and Zhao, 1993; Zhu and Chen, 1994).

5. Conclusion

In this study, we attempted to assess and map the desertification changes in the Hogno Khaan nature reserve in central Mongolia between 1990 and 2011 using Landsat images. Using calibration information with satellite data, all the images were radiometrically and atmospherically corrected using widely used techniques such as Dark-Object Subtraction (DOS). A combination of Decision Tree (DT) classification techniques were employed to derive maps for the observation period. These maps were combined with NDVI, TGSI, and land surface albedo generated by the DT method to derive final classification for each observation periods. The changes between pixels were then evaluated. A total of 928,321 pixels were tested, resulting in matrices of the desertification changes between 1990 and 2011.

The integrated desertification assessment by combining NDVI, TGSI and land surface albedo demonstrated a 87% difference in the desertified area between the three periods of the study (1990, 2002 and 2011). Overall, 15.3% of the area was subjected to land degradation (1990–2011), of which the severely degraded area increased by 8.1%, the medium degraded area decreased by 5.8%, and the low degraded area increased by 7.9%. Land degradation appeared mostly on sand dune, pastures and grassland areas. We also attempted to establish the desertification process by detecting changes in the surface NDVI, TGSI, and land

surface albedo distribution. In our study area, the highest TGSI values of 0.10–0.20 were found in areas of severe desertification.

Acknowledgments

We thank the editors and anonymous reviewers for their in-depth comments and review, which greatly improved this manuscript. This project was conducted with support from the Forest Science Technologies Development Project (Project Number: S211213L030320)" of the Korean Forest Service.

References

Bayasgalan, M. Monitoring of Drought in the Mongolia, 2005. Ulaanbaatar, Mongolia. Doctoral Dissertation.

Chavez, P.S.Jr. An improved dark-object subtraction technique for atmospheric scattering correction of multispectral data. Remote Sens Environ. 24, 459-479, 1988.

Chavez, P.S.Jr. Image-based atmospheric corrections – Revisited and improved. Photogram. Eng. Remote Sensing. 62, 1025-1036, 1996.

Dagmar Budikova, 2010. Albedo. www.eoearth.org/article/Albedo

Duanyang, Xu., Xiangwu Kang., Dongsheng Qiu., et al. Quantitative Assessment of Desertification Using Landsat Data on a Regional Scale – A Case Study in the Ordos Plateau, China. Sensors. 9, 1738-1753, 2009.

Dobos, E. Albedo. In: Lal, R. (Eds.), Encyclopedia of Soil Science, CRC Press, 2060 pp, 2003.

Friedl, M.A., Brodley, C. Decision tree classification of land cover from remotely sensed data. Remote Sens Environ. 61, 399-409, 1997.

Fu, H., Wang, Y., Wu, C., et al. Effects of grazing on soil physical and chemical properties of Alxa desert grassland. Journal of Desert Research. 22, 339-343, 2002.

Garcia Latorre, J., Garcia-Latorre, J., Sanchez-Picon, A. Dealing with aridity: socio-economic structures and environmental changes in an arid Mediterranean region, Land Use Policy.18, 53–64, 2001.

Hadeel, A.S., Mushtak, T.J, Chen, X. Remote sensing and GIS application in the detection of environmental degradation indicators. Geo-spatial information Science. 14, 39-47, 2010.

Jackson, R.D., Idso, S.B., Otterman, J. Surface albedo and desertification. Science. 189, 1012-1015, 1975.

Jensen, M.E., Burman, R.D., Allen, R.G. Evapotranspiration and irrigation water requirements. American Society of Civil Engineers. Rep. Pract. 70, 1990.

Jones, H.G. Plants and Microclimate: A Quantitative Approach to Environmental Plant Physiology. second Eds., Cambridge University Press, Cambridge, U.K, 1992.

Kassas, M., Rescuing drylands: a project of the world. Futures. 31, 949-958, 1999

Kotoda, K. Estimation of River Basin Evapotranspiration. Environmental. Research Center Papers, University of Tsukuba, 8, 1986.

Lal, R., Stewart, B.A. *Soil Degradation*, Springer Verlag, New York. 1990.

Liang, S.L. Narrowband to broadband conversions of land surface albedo I: Algorithms. Remote Sens Environ. 76, 213-238, 2001.

Li, S.G., Harazono, Y., Oikawa, T., et al. Grassland desertification by grazing and the resulting micrometeorological changes in Inner Mongolia. Agricultural and Forest Meteorology, 102, 125-137, 2000.

Liu, X.M., Zhao, H.L. Comprehensive Strategy for Eco-environmental Control in Horqin Sand Land. Gansu Science and Technology Publishing-house, Lanzhou, China, 88-115 (in Chinese), 1993.

Matthews, E. Vegetation, Land-Use and Seasonal Albedo Data Sets. In Global Change Data Base Africa Documentation, Appendix D, NOAA/NGDC. 1984.

Middleton, N., Thomas, D.S.G. World Atlas of Desertification. Arnold. pp. 182, 1997.

Michael Cherlet, Eva Ivits, Stefan Sommer, Gergely Tóth, Arwyn Jones, Luca Montanarella, Alan Belward, Towards a better understanding of land and soil degradation in Europe, 2012. UNCCD http://ec.europa.eu/environment/archives/soil/pdf/nov2012/121115-%20A.BELWARD%20Land%20and%20Soil%20degradation%20EU%20final.pdf

Mclver, D.K., Friedl, M.A. Using prior probabilities in decision-tree classification of remotely sensed data. Remote Sens. Envrion. 81, 253-261, 2002.

Musick, H.B. Temporal change of Landsat MSS albedo estimates in arid rangeland. Remote Sensing of Environment, 20, 107-120, 1986.

D'Odorico, P., Bhattachan, A., Davis, K.F., et al. Global desertification: Drivers and feedbacks. Advances in Water Resources. 51, 326-344, 2013.

Oke, T.R. Boundary Layer Climates, Methuen: New York, NY, pp. 464, 1978.

Pan, J., Qin, X. Extracting desertification from Landsat imagery using a feature space composed of vegetation index and albedo-a case study of Zhangye oasis and its adjacent areas. Science of Surveying and Mapping. 3, 193-195, 2010.

Puigdefabregas, J., Mendizabal, T. Perspectives on desertification: western Mediterranean, J. Arid Environ. 39, 209 - 224, 1998.

Riobinove, C.J., Chavez, P.S., Gehring, D., et al. Arid land monitoring using Landsat albedo difference images. Remote Sens Environ. 11, 133-156, 1981.

Rogan, J., Franklin, J., Roberts, D.A. A comparison of methods for monitoring multi temporal vegetation change using Thematic Mapper imagery. Remote Sens Environ. 80, 143-156, 2002.

Rubio, J.L. Recatala, L., The relevance and consequences of Mediterranean desertification including security aspects. In: Kepner, W.G., Rubio, J.L., Mouat,D.A. and Pedrazzini, F. (eds.), Desertification in the Mediterranean region : a security issue. Netherlands: Springer, pp, 133-165, 2006.

Smith, R.B. The heat budget of the earth's surface deduced from space. available on http://www.yale.edu/ceo/Documentation/ceo_faq.html, 2010.

Tucker, C.J. Red and photographic infrared linear combinations for monitoring vegetation. Remote Sens Environ. 8, 127-150, 1979.

United Nations. Desertification: Its Causes and Consequences. Pergamon Press, Oxford, UK, 1977.

Van Wijk, W.R., Scholte Using, D.W. Radiation. In: Van Wijk, W.R. (Eds.). Physics of Plant Environment. North- Holland Publishing Co.: Amsterdam, The Netherlands, pp. 62-101, 1963.

Vermote, E.F., D. Tanre, J.L. Deuze, M., et al. Second simulation of the satellite signal in the solar spectrum, 6S: An overview, IEEE Transactions on Geoscience and Remote Sensing. 35, 675–686, 1997b.

Xiao, J., Shen, Y., Tateishi, R., et al. Development of topsoil grain size index for monitoring desertification in arid land using remote sensing. International Journal of Remote Sensing. 27, 2411-2422, 2006.

Xiaohong Chen, Zhenghu Duan. Changes in soil physical and chemical properties during reversal of desertification in Yanchi County of Ningxia Hui autonomous region, China. Environ Geol, 57, 975–985, 2009.

Xu, D., Kang, X., Qiu, D., et al. Quantitative assessment of desertification using Landsat data on a regional scale – A case study in the Ordos Plateau, China. Sensors. 9, 1738-1753, 2009.

Zeng, Y., Xiang, N., Feng, Z., et al. Albedo-NDVI space and remote sensing synthesis index models for desertification monitoring. Scientia Geographical Sinica. 1, 75-81, 2006.

Zhao, H.L., Zhao, X.Y., Zhou, R.L., et al. Desertification processes due to heavy grazing in sandy rangeland, Inner Mongolia. Journal of Arid Environ. 1 - 1, 2005.

Zhang, T.H., Zhao H.L., Li, S.G., et al. A comparison of different measures for stabilizing moving sand dunes in the Horqin Sandy Land of Inner Mongolia, China**,** Journal of Arid Environments. 58, 2203-214, 2004.

Zhu, Z.D., Chen, G.T., Sandy Desertification in China Status and Trends. Science Press, Beijing, pp.250, (in Chinese), 1994.

Zhu, Z., Liu, S., Di, X., Desertification and its Rehabilitation in China (Beijing: China Science Press). 1989.

NASA's Giovanni project http://giovanni.gsfc.nasa.gov/giovanni/.

Figure captions

Figure 1. Geographic location of the study area (LANDSAT ETM (17.08.2011).

Figure 2. Graph of rainfall (1990-2014) and air temperature (2003-2014) of study area generated by NASA's Giovanni.

Figure 3. Tree diagram for assessing and classifying desertification grade using NDVI, TGSI, and albedo.

Figure 4. a) NDVI, b) TGSI, and c) albedo map for each year.

Figure 5. Slope of correlation between NDVI, TGSI, and albedo. a) Slope of correlation between NDVI and albedo. b) Slope of correlation between NDVI and TGSI. c) Slope of correlation between TGSI and albedo.

Figure 6. Desertification maps of Hogno Khaan protected area in 1990, 2002, and 2011.

Figure 7. Desertification change map between 1990 and 2011.